



**HAL**  
open science

## Water-level fluctuation enhances sediment and trace metal mobility in lake littoral

Nathalie Lécivain, Bernard Clément, Aymeric Dabrin, Juliette Seigle-Ferrand, Damien Bouffard, Emmanuel Naffrechoux, Victor Frossard

### ► To cite this version:

Nathalie Lécivain, Bernard Clément, Aymeric Dabrin, Juliette Seigle-Ferrand, Damien Bouffard, et al.. Water-level fluctuation enhances sediment and trace metal mobility in lake littoral. *Chemosphere*, 2021, 264 (2), pp.128451. 10.1016/j.chemosphere.2020.128451 . hal-03358554

**HAL Id: hal-03358554**

**<https://hal.science/hal-03358554>**

Submitted on 17 Oct 2022

**HAL** is a multi-disciplinary open access archive for the deposit and dissemination of scientific research documents, whether they are published or not. The documents may come from teaching and research institutions in France or abroad, or from public or private research centers.

L'archive ouverte pluridisciplinaire **HAL**, est destinée au dépôt et à la diffusion de documents scientifiques de niveau recherche, publiés ou non, émanant des établissements d'enseignement et de recherche français ou étrangers, des laboratoires publics ou privés.



Distributed under a Creative Commons Attribution - NonCommercial 4.0 International License

## **Water-level fluctuation enhances sediment and trace metal mobility in lake littoral**

Nathalie Lécivain<sup>1</sup>, Bernard Clément<sup>1</sup>, Aymeric Dabrin<sup>2</sup>, Juliette Seigle-Ferrand<sup>3</sup>, Damien Bouffard<sup>4</sup>,  
Emmanuel Naffrechoux<sup>5</sup>, Victor Frossard<sup>6</sup>✉

<sup>1</sup>Univ Lyon, Université Claude Bernard Lyon 1, CNRS, ENTPE, UMR5023 LEHNA, F-69518, Vaulx-en-Velin, France

<sup>2</sup>Irstea, UMR 5553 RiverLy, centre de Lyon-Villeurbanne, 69625 Villeurbanne Cedex, France

<sup>3</sup>UMR LECA, Université Savoie Mont-Blanc, 73376 Le Bourget du Lac, France

<sup>4</sup>Eawag, Swiss Federal Institute of Aquatic Science and Technology, Surface Waters - Research and Management, Kastanienbaum, Switzerland.

<sup>5</sup>UMR LCME, Univ. Savoie Mont-Blanc, 73000 Chambéry, France

<sup>6</sup>UMR 42 CARTELE, Université Savoie Mont-Blanc, 73376 Le Bourget du Lac, France

✉Corresponding author: [victor.frossard@univ-smb.fr](mailto:victor.frossard@univ-smb.fr)

1 **Abstract**

2 Water-level fluctuation (WLF) is a widespread management action in lakes and reservoirs whose  
3 impacts on contaminant fate have seldom been investigated. We used near shore hourly measurements  
4 (n = 2122) of turbidity (contaminant proxy) and water velocity (sediment resuspension proxy) to track  
5 high-frequency contaminant dynamics during a 0.6 m change in water level observed in autumn 2017  
6 in a large French lake. Simultaneously, discrete trace metal measurements highlighted that trapped  
7 sediment was more contaminated and finer than surficial sediment supporting that suspended particles  
8 (measured by turbidity) were a preferential medium for contaminant mobility. General additive models  
9 involving tensor products revealed the enhancement of wind-speed and river discharge effects on  
10 turbidity with water draw down. The decrease of the explained deviances by the models over time-lags  
11 indicated short time-scale response of turbidity to external forcing. Three of the four major turbid  
12 events occurred at the lowest water-level and were concomitant of sediment resuspension as well as  
13 precipitation events and / or river flood suggesting a complex interplay among in-lake and watershed  
14 processes at controlling sediment mobility during the WLF. These results shed in light that WLF can  
15 affect lake littoral hydrodynamic cascading up to the enhancement of contaminant mobility. Sediment  
16 resuspension may be an overlooked feature of WLF increasing contamination risk and exposure for  
17 littoral organisms with widespread ecological consequences due to the large number of water-level  
18 regulated ecosystems.

19

20 **Keywords**

21 water-level fluctuation, trace metals, turbidity, resuspension model, lake littoral

22

## 23 **1. Introduction**

24 The fate of contaminants in aquatic ecosystems depends on physical transport and mixing as well as  
25 geochemical processes both acting at different time scales that remain difficult to capture in the field.  
26 Discrete and passive sampling (e.g. Diffusive Gradient in thin film) provide time-average insights on  
27 local contamination yet masking real-time contaminant behavior (Lécrivain et al. 2018, Bretier et al.  
28 2019). Recent approaches such as electroanalytical methods progressively open the way for real-time  
29 monitoring of contaminants while their implementation remain currently limited to short time-scales  
30 (i.e. hours to days, Garnier et al. 2006) or necessitate stringent monitoring systems (Superville et al.  
31 2015). Contaminant bioavailability modeling accounting for physical and chemical characteristics of  
32 sediment, water and contaminant can make valuable predictions for an array of contaminants but  
33 necessitate a high number of parameters at work (e.g. partitioning coefficients) and still a consequent  
34 environmental monitoring (Di Toro et al. 2005; Paquin et al. 2002, Brix et al. 2017).

35 Alternatively, turbidity, measured as nephelometric turbidity units (NTU), is among the most basic  
36 environmental integrative information that can be recorded at high-frequency. It quantifies the  
37 cloudiness of water related to the amount of suspended particles that are a preferential medium for  
38 adsorbed contaminant (Chiffre et al. 2015; Kalnejais et al. 2007). The ability of particles to adsorb  
39 contaminant change with particle grain size due to changes in specific surface area (Martincic et al.  
40 1990) (Sutherland 2003) and suspended particles tend to contain much higher contamination than the  
41 bulk sediment they originate due to smaller grain size (Kalnejais et al. 2007). Turbidity can also  
42 inform on the dynamics of dissolved contaminants as soluble contaminant from soils or sediment  
43 generally co-occur with particle resuspension events (Cantwell et al. 2002; Fetters et al. 2016). For  
44 instance, Bretier et al. (2019) recently reported a sharp increase of Mn, Ni, Co and As dissolved  
45 concentrations concomitantly with high suspended particulate matter (i.e. high turbidity) triggered by  
46 sediment release from a dam flushing event in the Upper Rhône River. Consequently, the  
47 consideration of the size of suspended particles in complement to turbidity (i.e. the overall particle  
48 concentration) could provide valuable indicators for tracking contaminant fate in freshwaters overtime.  
49 Rather than estimating the actual contamination that can be obtained by relevant discrete sampling,

50 these indicators could enable the assessment of the relative changes in contaminant mobility and  
51 ultimately biota exposure to contaminant overtime (Weltens et al. 2000).

52 We investigated high-frequency (hourly measurements) dynamics of littoral turbidity and water  
53 velocity along with external forcing (i.e. precipitation, wind speed, river discharge) during a water-  
54 level fluctuation event (WLF,  $\Delta$ depth = 60 cm) that occurred in autumn 2017 in the largest natural  
55 French lake (Lake Bourget). A sediment resuspension model quantifying the occurrence of grain size-  
56 specific sediment resuspension events was derived from water velocity (Soulsby and Whitehouse  
57 1997, Graham et al. 2016). Complementarily, discrete measurements of trace metals (TM) were  
58 performed at three occasions (before-during-after WLF) among two different matrices (surficial and  
59 trapped sediments) to assess the actual contamination of the littoral and its possible variation during  
60 the WLF.

61 The overarching aim of this study was to evaluate the dynamic of suspended particles (i.e. turbidity) as  
62 a proxy for TM dynamic during the WLF tackled through the following working hypotheses:

- 63 1) The low water-level during the WLF should foster wind-induced sediment resuspension  
64 (Cózar et al. 2005; Hofmann et al. 2008), increasing turbidity and metal mobility.
- 65 2) The effects of external forcing on turbidity should modulate by the WLF and increased for low  
66 water-level.
- 67 3) The occurrence of high turbidity events should be associated to sediment resuspension events  
68 indicating that in-lake processes may be responsible for turbidity. Alternatively, watershed  
69 processes (i.e. export of suspended particles) should be involved.

70 Overall, these investigations were expected to provide insights regarding the influence of WLF on  
71 contaminant dynamics, an often overlooked feature of WLF within lake littorals.

72

## 73 2. Materials and methods

### 74 2.1. Lake Bourget and study sites

75 Lake Bourget is the largest French natural lake (44.5 km<sup>2</sup>, 45.43°58.2'N 5°51'59.1'E) sheltered within  
76 the limestone mountains of the Epine and Bauges. The catchment area of the lake is 560 km<sup>2</sup> and  
77 covered by forests (45 %), agricultural areas (22 %), grazing fields (12 %), urban areas (13 %) and  
78 water bodies (8 %) (CISALB 2009). The littoral sediment contained by a mixture of contaminants  
79 exerting low but heterogeneous toxicity. Higher contaminant concentrations were reported in the  
80 southeastern region of the lake mostly resulting from local watershed run-offs (Lécrivain et al. 2018;  
81 Lécrivain et al. 2019). We selected this southeastern region for the study area. This area is  
82 characterized by a ~ 5 % gentle slope close to the outlet of a small arm of the Tillet River, one of the  
83 main tributary of the lake (45°40'00.6"N 5°53'39.0"E) (Appendix 1). Three study sites distant of 20 m  
84 to each other were retained along a littoral transect (Appendix 1). The shallowest site (S<sub>0.7</sub>) was  
85 located ~ 10 m away from the shoreline at 0.7 m depth and the two other points (S<sub>1.5</sub> and S<sub>2.5</sub>) at ~ 30  
86 m and ~ 50 m from the shoreline at depths of 1.5 m and 2.5 m respectively. The experimental design as  
87 well as physico-chemical monitoring among the study sites are presented in Appendix 2.

### 88 2.2. Trace metal contamination

89 TM discrete measurements were performed at three temporal steps over the WLF. On the 2017/08/31,  
90 step 1 provided information before the water-level dropped down. On 2017/10/19, step 2 provided  
91 information at the lowest level. Finally, on 2018/04/24, step 3 provided information resulting from the  
92 water-level increase (step 3).

93 Triplicates of TM measurements were performed at each site among two different matrices: surficial  
94 and trapped sediments. Sediment traps were deployed two weeks prior sampling sessions to ensure  
95 sediment accumulation. After sampling, the surficial and trapped sediments were placed in pre-washed  
96 polyethylene bottles, transported to the laboratory in coolers, sieved at 2 mm to remove macro-debris  
97 and stored at 4°C during a maximum of 24 hours.

98 Prior to the measurements, bulk sediments were mineralized in a microwave oven (CEM/MARS  
99 Xpress, 2 mL of ultra-pure HNO<sub>3</sub> + 6 mL of ultra-pure HCl, 180 °C for 30 min, filtration on a 0.45-

100  $\mu\text{m}$  Whatman<sup>TM</sup> filter and dilution of the residue in 25 mL of ultra-pure water). The sediment grain  
101 size spectra were quantified using a Malvern Mastersizer 2000G. TM concentrations were then  
102 estimated by atomic absorption spectrometry (AAS). The total sediment contents of Cd, Cr, Cu, Ni  
103 and Pb were measured in a graphite furnace at 1500 °C, and the total sediment content of Zn was  
104 measured with an air-acetylene flame (Perkin Elmer, model PinAAcle 900T). The detection limits  
105 were as follows: Cd = 2.5  $\mu\text{g kg}^{-1}$  DM, Cr = 10  $\mu\text{g kg}^{-1}$  DM, Cu = 3.5  $\mu\text{g kg}^{-1}$  DM, Ni = 17.5  $\mu\text{g kg}^{-1}$   
106 DM, Pb = 12.5  $\mu\text{g kg}^{-1}$  DM, Zn = 375  $\mu\text{g kg}^{-1}$  DM. Certified reference material (River sediment LGC6  
107 187) was used for standardization, and triplicate measurements were done to ensure that analytical  
108 errors were under 2%.

### 109 *2.3. Turbidity and external forcings*

110 Water turbidity was measured at hourly frequency using an Aqua Troll 600 multiparameter probe  
111 located at site S<sub>1.5</sub> to quantify the amount of particles present in the open water. We performed 2-point  
112 calibration at 10 NTU and 100 NTU for turbidity measurements using In Situ's turbidity standards and  
113 a new calibration was performed at the beginning of each new step. Hourly measurements for wind  
114 speed and precipitation were collected from the meteorological station of Météo-France Chambéry-  
115 Aix-73329001 (Appendix 3). Hourly discharges of the Leysse River were extracted from the national  
116 station of La Motte-Servolex-V1315020 (<http://hydro.eaufrance.fr/>, Appendix 3). The flood plume of  
117 the Leysse River typically flows North-East toward the studied area (Vinçon-Leite et al. 1998) and the  
118 discharges of both the Leysse River and the Tillet River (nearby the study area) exhibit similar  
119 hydrological regimes and only information from the Leysse River were considered here.

### 120 *Sediment resuspension model*

121 The local sediment resuspension was quantified by the dimensionless Shields mobility parameter ( $\theta$ ,  
122 Soulsby and Whitehouse 1997). The Shields parameter was derived by combining sediment  
123 information (modal grain size and density) with water current velocity data obtained at site S<sub>2.5</sub> with an  
124 acoustic Doppler current profiler (ADCP, AQUADOPP Profiler 2MHz) set up for recording hourly

125 velocity over 2 m depth. We used velocity data at 70 cm above the sediment. This height was chosen  
126 as an optimal distance from the bottom where the logarithmic velocity profile is well developed.

127 The dimensionless mobility Shields parameter is obtained as follows:

$$128 \quad \theta = \frac{\tau_b}{(\rho_s - \rho_w) \times g \times d} \quad (1)$$

129 where  $\tau_b$  is the bottom shear stress ( $\text{kg m}^{-1}\text{s}^{-2}$ ),  $\rho_s$  is the particle density ( $2600 \text{ kg m}^{-3}$ ),  $\rho_w$  is the water  
130 density at the sediment surface ( $1000 \text{ kg m}^{-3}$ ),  $g$  is the gravitational acceleration ( $9.81 \text{ m s}^{-2}$ ) and  $d$  is  
131 the sediment mean particle diameter (taken as the modal lake and trapped sediment particle sizes of  
132  $159 \text{ }\mu\text{m}$  and  $127 \text{ }\mu\text{m}$  respectively, Appendix 4).

133 The bottom shear stress ( $\tau_b$ ) represents the product of water density and the square of the shear bed  
134 velocity ( $u_*$ ):

$$135 \quad \tau_b = \rho_w \times u_*^2 \quad (2)$$

136 The bottom shear stress is estimated using the water current velocity data,  $U$  ( $\text{m s}^{-1}$ ), assuming a  
137 logarithmic velocity profile above the sediment bed:

$$138 \quad u_* = \frac{k \times U(z)}{\ln\left(\frac{z}{z_0}\right)} \quad (3)$$

139 where  $z$  is the distance between the sediment and the current velocity measured by the ADCP in  
140 meters (here  $70 \text{ cm}$ ),  $k$  is the von Karman's constant ( $0.4 \text{ m s}^{-1}$ ),  $z_0$  is the roughness height ( $5 \times 10^{-3}$   
141  $\text{m}$ , Bouffard and Lemmin 2013).

142 In order to estimate the resuspension potential of the sediment particles, the Shields parameter was  
143 confronted to a dimensionless critical value ( $\theta_{cr}$ ), above which sediment resuspension was expected  
144 according to (Soulsby and Whitehouse 1997) as follows:

$$145 \quad \theta_{cr} = \frac{0.3}{1+1.2 \times D_*} + 0.055 \times (1 - \exp^{-0.02 D_*}) \quad (4)$$

146 where the dimensionless grain size ( $D_*$ ) is expressed as follows:

$$147 \quad D_* = d \sqrt{\frac{3 \times g \times (\frac{\rho_s}{\rho_w} - 1)}{v^2}} \quad (5)$$

148 where  $v$  is the kinematic viscosity ( $\text{m}^2 \text{ s}^{-1}$ ).

149 *2.5. Statistical analyses*

150 Mann-Whitney tests were used to estimate the significance of the difference in TM concentrations  
151 among surficial and trapped sediment. Generalized additive models (GAM, Hastie and Tibshirani  
152 1990, Wood 2006) were selected to analyze the relationships between turbidity and the external  
153 forcing. GAMs are flexible non-parametric models that accommodate for nonlinear relationships  
154 between variables and can support different distributions of the response variable. The extent of  
155 nonlinear relationship among variables is quantified through the estimated degree of freedom (edf)  
156 where edf = 1 indicate linear relationship and edf higher than 1 indicate progressively higher nonlinear  
157 relationship. A first GAM was computed considering water pressure as single variable to identify the  
158 general influence of WLF on turbidity. A second GAM that considered the three external forcing was  
159 fitted to assess their respective influence on turbidity. A last GAM involving tensor product smooths  
160 (Wood 2006) was finally fitted to address the possible modulation of WLF on the relationships  
161 between turbidity and the external forcing. The tensor product smooths allow the smooth relationship  
162 between turbidity and the external forcing to change nonlinearly with WLF. The tensor product  
163 interaction terms in the GAM reflected how the relationship between turbidity and the external forcing  
164 can be modulated by WLF. Tensor product interaction terms are suitable to model responses to  
165 interactions of variables with different units, which is the case in this study, and have been shown to  
166 provide fruitful insight among complex ecological interactions (e.g. Bachelier et al. 2009, Kvile et al.  
167 2016). The possible time-lag response of turbidity to the external forcing was investigated by fitting  
168 the last GAM with delayed external forcing from 0 to 48 hours (i.e. responses variables were modeled  
169 against external forcing previously recorded from 0 hour (instantaneous) to 48 hours). We considered  
170 four knots and cubic regression splines to construct the smoothing splines and fitting the GAM and  
171 their performances were assessed by the proportion of deviance explained. Turbidity was  $\log_{10}$ -  
172 transformed prior the analyses and a Gamma distribution was considered for  $\log_{10}$ -transformed  
173 turbidity as it was a continuous variable bounded down 0 and clearly diverging from a normal  
174 distribution due to its right-skewness.

175 All statistical analyses as well as graphical displays were performed using R 3.6.3 (R Development  
176 Core Team 2020) and the packages *mgcv* (Wood and Augustin 2002, Wood 2006), *ggplot2* (Wickham  
177 2009).

### 178 3. Results

#### 179 3.1. WLF, turbidity and water velocity dynamics

180 The water level drawdown started in September, stabilized during October and was followed by the w  
181 ater level increase in November (Fig. 1A). Over the three-months survey, background turbidity was m  
182 ostly below 10 NTU (Fig. 1B). We however distinctly identified four major turbid events occurred (i.e  
183 . > 100 NTU, maximum turbidity ~ 3500 NTU) spanning from few days to several weeks (Fig. 1B). W  
184 ater velocity was low over most of the study period (i.e. < 0.05 cm s<sup>-1</sup>) and short higher velocity events  
185 were punctually recorded both in September and October with intensity reaching up to 0.15 cm s<sup>-1</sup> (Fig  
186 . 1C). During the two first weeks of November, the water velocity was more fluctuating and reached hi  
187 gher level than during the previous months and the highest water velocity of 0.18 cm s<sup>-1</sup> was recorded.

#### 188 3.2. Trace metal contamination

189 Surficial and trapped sediments mostly corresponded to fine sand according to Wentworth's (1922)  
190 classification although they differed in the mode values of grain size with surficial sediment being  
191 coarser (159 μm) than the trapped one (127 μm) (Appendix 4). Most TM significantly differed among  
192 these two types of sediment with concentration significantly higher for the trapped sediment than for  
193 the surficial one except for Cr and Ni that did not exhibit significant differences in their TM  
194 concentration (Fig. 2). When significant, the extent of TM enrichment for trapped sediment compared  
195 to the surficial one varied among TM from ~ 15 % enrichment for Cd to ~ 100 % enrichment for Cu.

#### 196 3.3. Turbidity, WLF and external forcings

197 The univariate GAM highlighted significant changes in turbidity along with WLF (Fig. 3A, Table 1).  
198 The pattern was nonlinear with an overall increase in turbidity with decreasing water level.  
199 Differently, a multivariate GAM indicated that turbidity did not significantly varied with precipitation  
200 but significantly linearly increased with both wind speed and river discharge (Fig. 3B to D, Table 1).  
201 Nevertheless, this multivariate GAM explained a limited proportion of the overall turbidity variability  
202 (i.e. 5.3% of the total deviance). A multivariate GAM accounting for the interactions between WLF  
203 and the significant external forcing was then fitted and its explanatory power was greatly higher (i.e.

204 35.2 % of the total deviance) than without considering interaction with WLF (Table 1, Fig. 4). This  
205 feature highlighted the role of external forcing on turbidity by WLF. The effect of wind speed  
206 appeared stronger at low water levels with higher slope compared to higher water levels (Fig. 4A).  
207 Similarly, the positive and nonlinear relationship linking discharge and turbidity was identified for low  
208 water levels while it was nonlinearly negative at high water levels (Fig. 4B). For both external forcing  
209 the higher predicted turbidity was identified for the lower water levels.

210 The multivariate GAM accounting for WLF interaction was fitted for increasing time-lags of the  
211 external forcing (Fig. 5). The proportion of deviance explained remained steady for the five first time-  
212 lags prior decreasing progressively up to 48h time-lags. The explanatory power of the multivariate  
213 GAM was hence the highest when considering no or short-term delay for the external forcing.

#### 214 3.4. Resuspension events

215 Over the three months of the study, the mean water velocity was  $3 \pm 2 \text{ cm s}^{-1}$  with several episodic eve  
216 nts reaching velocity of about  $15 \text{ cm s}^{-1}$  and a maximal velocity of  $18 \text{ cm s}^{-1}$  by mid-November (Fig. 6  
217 A). These results shed in light the highly hydrodynamic constraints of the littoral of this large lake. Th  
218 e water velocity allowed computing the Shield parameter informing of the initiation of sediment resus  
219 pension for specific sediment grain sizes (Fig. 6B). When considering the mode value of surficial sedi  
220 ment grain size, three sediment resuspension events occurred over the studied period. By the end of Se  
221 ptember, the first resuspension event was not related to a turbid event while for the second and third re  
222 suspension events the onsets of turbid events could be identified. Three complementary sediment resus  
223 pension events would occur considering mode of trapped sediment (Fig. 6B). The first one was conco  
224 mitant with the onset of the longer turbid event spanning from the end of October to early November a  
225 nd by the end of this turbid event a second resuspension event was suggested by the Shield parameter.  
226 The third resuspension event for the mode of trapped sediment occurred close to the last resuspension  
227 event for lake sediment mode values during the third turbid event. Considering the water velocity reco  
228 rded during the studied period, the number of resuspension events decreased exponentially with sedim  
229 ent grain size (Fig. 6C). The highest sediment grain size that could be resuspended (i.e. a single resusp  
230 ension event) had a diameter of  $230 \mu\text{m}$  and the number of resuspension events started to sharply incre  
231 ase for sediment finer than  $50 \mu\text{m}$  diameter.



## 233 4. Discussion

### 234 4.1. Turbidity as a contaminant proxy

235 Turbidity was especially variable over the study period and three of the four major turbid events  
236 recorded occurred during the lowest water-level period while the overall positive effect of water  
237 drawdown on turbidity could be more precisely quantified using a GAM. These results enabled to  
238 validate the hypothesis of an increasing turbidity as long as the water-level was lowered during the  
239 WLF. Further, the higher TM concentrations measured in trapped sediment compared to those in  
240 surficial sediment, likely related to their finer grain-size spectra (Martincic et al. 1990; Zhang et al.  
241 2002, Sutherland 2003), supported the hypothesis that suspended particles were a preferential medium  
242 for TM mobility. Turbidity could hence be a relevant proxy to inform of the amount of TM within the  
243 open-water of lake littoral (Yao et al. 2016, Nasrabadi et al. 2016). As a consequence, WLF may foster  
244 TM exposure of the littoral biota as along with particle-adsorbed TM, dissolved TM have been shown  
245 to increase with turbidity (Brétier et al. 2019). The contamination risk of TM for the littoral biota  
246 would be enhanced during the lowest water-levels of WLF representing an adverse effect on littoral  
247 organisms of this management action. Complementary investigations such as TM sequential extraction  
248 (Lécrivain et al. 2019) and / or quantifying TM dissolved concentrations may complement our  
249 approach to better decipher TM exposure and their bioavailability for the littoral biota (Eggleton and  
250 Thomas 2004, Atkinson et al. 2007; Fetters et al. 2016, Nasrabadi et al. 2018).

### 251 4.2. Modulation of turbidity by water-level fluctuation

252 Among the external forcings considered, wind speed and river discharge had significant positive  
253 effects on turbidity yet their explanatory power (i.e. deviance explained) remained limited when  
254 considered additively. Their positive influence on turbidity was expected as both wind speed and  
255 discharge can either trigger sediment resuspension (Zheng et al. 2013) or support the input of  
256 sediments from the watershed (Hofmann et al. 2008) and two main reasons may explain their limited  
257 explanatory power. First, these measurements were performed at the closest long term monitoring  
258 stations from the studied sites (i.e. a distance of few km) possibly limiting the accuracy of these

259 variables actually acting at the study area. Second, other factors that were not accounted for such as  
260 upwelling may also have been involved in littoral variation of turbidity. Accounting for the  
261 interactions of wind speed and river discharge with WLF through the use of the tensor products in  
262 GAM to model their effects on turbidity drastically increased the explanatory power of the GAM. This  
263 result indicated that WLF would effectively modulate the effects of external forcings on turbidity.  
264 More precisely the water drawdown increased the effects of the external forcings on turbidity which  
265 amplifies the amount of suspended particles highlighting direct influence on WLF on contaminant  
266 mobility.

267 The decrease of deviance explained by the GAM over successive time lags suggested short time-scale  
268 (i.e. hours) response of turbidity to the external forcings. This result supports the relevance for  
269 considering high-frequency measurements to address contaminant mobility in lake littoral.  
270 Complementarily, the maintaining of rather high deviance explained at larger time-lags indicated that  
271 the external forcings may still influence turbidity at longer time-scale (i.e. several days). This result is  
272 in accordance with the sinking speed of sediment modal grain size that may be of several days  
273 considering turbulent regime in the lake littoral (Appendix 5). In other words, the external forcings  
274 would almost instantaneously affect particle and contaminant mobility that would maintain (i.e.  
275 delayed effect) for several days which constitutes suitable conditions for biota exposure to  
276 contaminant.

#### 277 4.3. Linking turbidity to in-lake processes

278 The lake littoral supported high hydrodynamic constraints as shown by the bottom water velocity that  
279 regularly exceeded  $10 \text{ cm s}^{-1}$  corresponding to shear stress higher than  $10 \text{ N m}^{-2}$  with maximal values  
280 of  $\sim 20 \text{ N m}^{-2}$  (Appendix 6). Such hydrodynamic constraint was of similar magnitude than those  
281 reported by Kalnejais et al. (2007) in the Boston Harbor (USA) for which resuspension events due to  
282 shear stress contributed up to 60% of the flux of resuspended metal in an average year. The  
283 resuspension events increased exponentially as long a sediment grain size decreased with a major  
284 inflexion at  $\sim 50 \mu\text{m}$  grain size in diameter. This result may be linked to the noisy variations of low  
285 turbidity outside of the major turbid events and explain the grain size spectra of the littoral sediment

286 (Appendix 4) whose fraction smaller than 100  $\mu\text{m}$  in diameter drastically decreased. The lake littoral  
287 hence primarily acts as a transport area for fine sediment to storage compartments in deeper zones  
288 (Morales-Marin et al. 2018). This assertion is supported by the finer particle size of deep sediment  
289 compared to littoral ones often associated to higher contaminant concentrations.

290 The major turbid events were mostly associated to sediment resuspension events when considering  
291 mode values of trapped and surficial sediment indicating that in-lake processes involving bottom shear  
292 stress may explain their onsets. However, most turbid events were also concomitant of high river  
293 discharge or precipitation suggesting that watershed processes (i.e. particle export from the watershed)  
294 would also be involved in the turbidity variations. For instance, the longest turbid event of several  
295 weeks that started by mid-October was associated to a unique resuspension event for the mode of  
296 trapped sediment and its duration may then not been only attributable only to in-lake process  
297 supporting lake sediment remobilization. The complex interplay between in-lake and watershed  
298 processes likely control the onset and duration of turbid events whose relative implication likely varied  
299 among turbid events ultimately constraining contaminant mobility. This complexity was tentatively  
300 addressed using the GAM considering wind speed (i.e. in-lake process) and river discharge (i.e.  
301 watershed process) that may provide useful forecast for turbidity dynamic within the littoral of this  
302 large natural French lake.

### 303 **Conclusion**

304 We showed that WLF may significantly modulate the influence of the external forcing that drove the  
305 littoral turbidity. The enhancement of turbidity for the lowest water level associated to higher TM  
306 contamination of resuspended sediment provided evidence of the influence of WLF on TM mobility.  
307 Biota exposure may hence be amplified as ingestion of suspended contaminated particles is a common  
308 contamination pathway for both benthic and pelagic consumers (Weltens et al. 2000, Li et al. 2017)  
309 along with passive contamination via dissolved contaminant assimilation. Overall, turbidity may be a  
310 suitable proxy for high-frequency monitoring in complement to discrete contaminant measurements in  
311 highly dynamic aquatic ecosystems such as lake littoral. Due to the large number of water-level  
312 regulated ecosystems affected by WLF and in the perspective of their increasing establishment

313 (Farinotti et al. 2019), the effects of WLF on contaminant fate may have underestimated indirect and  
314 delayed impacts on littoral biodiversity compared to direct and more commonly reported alterations  
315 (Carmignani and Roy 2017; Evtimova and Donohue 2014).  
316

317

318 **Acknowledgment**

319 We thank AnaEE-France (Analyses et Expérimentations sur les Ecosystèmes - France) for their  
320 financial support for the acquisition of the acoustic Doppler current profiler and the Comité  
321 Intercommunautaire pour l'Assainissement du Lac du Bourget (especially Sébastien Cachera) for their  
322 constructive discussions regarding the water-level fluctuation on Lake Bourget. We are grateful to two  
323 anonymous reviewers for their constructive suggestions that improved the early version of the  
324 manuscript.

325

326 **References**

- 327 Atkinson, C. A., Jolley, D. F., Simpson, S. L., 2007. Effect of overlying water pH, dissolved oxygen,  
328 salinity and sediment disturbances on metal release and sequestration from metal  
329 contaminated marine sediments. *Chemosphere*. 69, 1428-1437.
- 330 Bachelier, N. M., Bailey, K. M., Ciannelli, L., Bartolino, V., Chan., K.S., 2009. Density-dependent,  
331 landscape, and climate effects on spawning distribution of walleye pollock *Theragra*  
332 *chalcogramma*. *Mar. Ecol. Prog. Ser.* 391, 1-12.
- 333 Bretier, M., Dabrin, A., Bessueille-Barbier F., Coquery, M., 2019. The impact of dam flushing event  
334 on dissolved trace elements concentrations: Coupling integrative passive sampling and  
335 discrete monitoring. *Sci. Total Env.* 656, 433-446.
- 336 Brix, K. V., DeForest, D. K., Tear, L., Grosell M., Adams W. J., 2017. Use of Multiple Linear  
337 Regression Models for Setting Water Quality Criteria for Copper: A Complementary  
338 Approach to the Biotic Ligand Model. *Environ Sci Technol* 51, 5182-5192.
- 339 Carmignani, J. R., Roy, A. H., 2017. Ecological impacts of winter water level drawdowns on lake  
340 littoral zones: a review. *Aquat. Sci.* 79, 803-824.
- 341 Chiffre, A., Degiorgi, F., Morin-Crini, N., Bolard, A., Chanez E., Badot, P.-M., 2015. PAH occurrence  
342 in chalk river systems from the Jura region (France). Pertinence of suspended particulate  
343 matter and sediment as matrices for river quality monitoring. *Env. Sci. Poll. Res.* 22, 17486-  
344 17498.
- 345 CISALB, 2009. Contrat de bassin versant du Lac du Bourget. Rapport Comité Intersyndical pour  
346 l'Assainissement du Lac du Bourget. 104.
- 347 Cózar, A., Gálvez, J. A., Hull, V., García C. M., Loiselle, S. A., 2005. Sediment resuspension by wind  
348 in a shallow lake of Esteros del Iberá (Argentina): a model based on turbidimetry. *Ecol. Mod.*  
349 186, 63-76.
- 350 Di Toro, D. M., McGrath, J. A., Hansen, D. J., Berry, W. J., Paquin, P. R., Mathew, R., Wu K. B.,  
351 Santore, R. C., 2005. Predicting sediment metal toxicity using a sediment biotic ligand model:  
352 methodology and initial application. *Environ. Toxicol. Chem.* 24, 2410-2427.

353 Eggleton, J., Thomas, K. V., 2004. A review of factors affecting the release and bioavailability of  
354 contaminants during sediment disturbance events. *Env. Inter.* 30, 973-980.

355 Evtimova, V. V., Donohue, I., 2014. Quantifying ecological responses to amplified water level  
356 fluctuations in standing waters: an experimental approach. *J. Appl. Ecol.* 51, 1282-1291.

357 Farinotti, D., Round, V., Huss, M., Compagno L., Zekollari, H., 2019. Large hydropower and water-  
358 storage potential in future glacier-free basins. *Nature* 575, 341-344.

359 Fetters, K. J., Costello, D. M., Hammerschmidt C. R., Burton Jr., G. A., 2016. Toxicological effects of  
360 short-term resuspension of metal-contaminated freshwater and marine sediments. *Environ.*  
361 *Toxicol. Chem.* 35, 676-686.

362 Garnier, C., Lesven, L., Billon, G., Magnier, A., Mikkelsen Ø., Pižeta, I., 2006. Voltammetric  
363 procedure for trace metal analysis in polluted natural waters using homemade bare gold-disk  
364 microelectrodes. *Anal Bioanal. Chem.* 386, 313-323.

365 Graham, N. D., Bouffard D., Loizeau, J.-L., 2016. The influence of bottom boundary layer  
366 hydrodynamics on sediment focusing in a contaminated bay. *Environ. Sci. Pollut. Res.* 23,  
367 25412-25426.

368 Hastie, T., Tibshirani, R., 1990. *Generalized Additive Models*. London: Chapman and Hall.

369 Hofmann, H., Lorke, A., Peeters, F., 2008. Temporal scales of water-level fluctuations in lakes and  
370 their ecological implications. *Hydrobiologia* 613, 85-96.

371 Kalnejais, L. H., Martin, W. R., Signell R. P., Bothner, M. H., 2007. Role of Sediment Resuspension  
372 in the Remobilization of Particulate-Phase Metals from Coastal Sediments. *Environ. Sci.*  
373 *Technol.* 41, 2282-2288.

374 Kvile, K., Stige, L., Prokopchuk, I., Langangen, Ø., 2016. A statistical regression approach to estimate  
375 zooplankton mortality from spatiotemporal survey data. *J. Plankt. Res.* 38, 624-635.

376 Lécirvain, N., Aurenche, V., Cottin, N., Frossard V., Clément, B., 2018. Multi-contamination (heavy  
377 metals, polychlorinated biphenyls and polycyclic aromatic hydrocarbons) of littoral sediments

378 and the associated ecological risk assessment in a large lake in France (Lake Bourget). *Sci.*  
379 *Total Environ.* 619–620, 854-865.

380 Lécivain, N., Frossard, V., Naffrechoux, E., Clément, B., 2019. Looking at Organic Pollutants (OPs)  
381 Signatures in Littoral Sediments to Assess the Influence of a Local Urban Source at the Whole  
382 Lake Scale. *Polycycl. Aromat. Compd.* 1-13, doi:10.1080/10406638.2019.1631195.

383 Lécivain, N., Frossard, V., Clément, B. 2019. Changes in mobility of trace metals at the sediment-  
384 water-biota interfaces following laboratory drying and reimmersion of a lacustrine sediment.  
385 *Environ. Sci. Pol. Res.* 26, 14050-14058

386 Li, X., Peng, W., Jiang, Y., Duan, Y., Ren, J., Liu Y., Fan, W., 2017. The *Daphnia magna* role to  
387 predict the cadmium toxicity of sediment: Bioaccumulation and biomarker response. *Ecotox.*  
388 *Environ. Safe.* 138, 206-214.

389 Martincic, D., Kwokal Z., Branica, M., 1990. Distribution of zinc, lead, cadmium and copper between  
390 different size fractions of sediments I. The Limski Kanal (North Adriatic Sea). *Sci. Total.*  
391 *Environ.* 95, 201-215.

392 Morales-Marin, L. A., French, J. R., Burningham, H., Battarbee, R. W., 2018. Three-dimensional  
393 hydrodynamic and sediment transport modeling to test the sediment focusing hypothesis in  
394 upland lakes. *Limnol. Oceanogr.* 63, S156-S176.

395 Nasrabadi, T., Ruegner, H., Schwientek, M., Bennett, J., FazelValipour S. Grathwohl, P.,  
396 2018. Bulk metal concentrations versus total suspended solids in rivers: Time-invariant  
397 & catchment-specific relationships. *PLoS ONE* 13:e0191314.

398 Nasrabadi, T., Ruegner, H., Sirdari, Z. Z., Schwientek M., Grathwohl, P., 2016. Using total  
399 suspended solids (TSS) and turbidity as proxies for evaluation of metal transport in  
400 river water. *Applied Geochem.* 68, 1-9.

401 Paquin, P. R., Gorsuch, J. W., Apte, S., Batley, G. E., Bowles, K. C., Campbell, P. G. C., Delos, C. G.,  
402 Di Toro, D. M., Dwyer, R. L., Galvez, F., Gensemer, R. W., Goss, G. G., Hogstrand, C.,

403 Janssen, C. R., McGeer, J. C., Naddy, R. B., Playle, R. C., Santore, R. C., Schneider, U.,  
404 Stubblefield, W. A., Wood C. M., Wu, K. B., 2002. The biotic ligand model: a historical  
405 overview. *Comparative Biochemistry and Physiology Part C: Toxicol. Pharmacol.* 133, 3-35.

406 R Development Core Team, 2020. R: A language and environment for statistical computing. R  
407 Foundation for Statistical Computing. Vienna, Austria ISBN 3-900051-07-0, URL  
408 <http://wwwR-project.org/>.

409 Soulsby, R. L., Whitehouse, R. J. S., 1997. Threshold of Sediment Motion in Coastal Environments.  
410 In: *Pacific Coasts and Ports '97: Proceedings of the 13th Australasian Coastal and Ocean*  
411 *Engineering Conference and the 6th Australasian Port and Harbour Conference; Volume 1*  
412 *Christchurch, NZ: Centre for Advanced Engineering, University of Canterbury.* 145-150.

413 Superville, P.-J., Prygiel, E., Mikkelsen O., Billon, G., 2015. Dynamic behaviour of trace metals in the  
414 Deûle River impacted by recurrent polluted sediment resuspensions: From diel to seasonal  
415 evolutions. *Sci. Total. Environ.* 506-507, 585-593.

416 Sutherland, R. A., 2003. Lead in grain size fractions of road-deposited sediment. *Environ. Pollut.* 121,  
417 229-237.

418 Vinçon-Leite, B., Bournet, P. E., Gayte, X., Fontvieille D., Tassin, B., 1998. Impact of a flood event  
419 on the biogeochemical behaviour of a mesotrophic alpine lake: Lake Bourget (Savoy).  
420 *Hydrobiologia.* 373, 361-377.

421 Weltens, R., Goossens, R., Van Puymbroeck, S., 2000. Ecotoxicity of Contaminated Suspended Solids  
422 for Filter Feeders (*Daphnia magna*). *Arch. Environ. Con. Tox.* 39, 315-323.

423 Wickham, H., 2009. *ggplot2: Elegant Graphics for Data Analysis.* Springer-Verlag New-York.

424 Wood, S. Augustin, N., 2002. GAMs with integrated model selection using penalized regression  
425 splines and applications to environmental modelling. *Ecol. Model.* 157, 157-177.

426 Wood, S. N., 2006. *Generalized Additive Models: An Introduction with R.* Chapman & Hall, London.

427 Yao, H., W. Zhuang, Y. Qian, B. Xia, Y. Yang & X. Qian, 2016. Estimating and Predicting Metal  
428 Concentration Using Online Turbidity Values and Water Quality Models in Two Rivers of the

429 Taihu Basin, Eastern China. PloS one 11(3):e0152491-e0152491  
430 doi:10.1371/journal.pone.0152491.

431 Zhang, C., Wang, L., Li, G., Dong, S., Yang, J., Wang, X., 2002. Grain size effect on multi-element  
432 concentrations in sediments from the intertidal flats of Bohai Bay, China. *Appl. Geochem.* 17,  
433 59-68.

434 Zheng, S., Wang, P., Wang, C., Hou, J., Qian, J., 2013. Distribution of metals in water and suspended  
435 particulate matter during the resuspension processes in Taihu Lake sediment, China. *Quat. Int.*  
436 286, 94-102.

1 Tables

2

3

4 Table 1: Summary statistics of the GAMs considering only WLF and accounting or not for the WLF in  
5 combination with external forcings (i.e. tensor product smooths) to explain turbidity variability.

Variables	Smooth terms	edf	p-value	Deviance explained
WLF	s(Water-level)	3.0	<0.001	18 %
Forcings without WLF	s(Precipitation)	1.2	0.24	5.3 %
	s(Wind_speed)	1.0	<0.001	
	s(Discharge)	1.0	<0.001	
Forcings accounting for WLF	te(Wind_speed, water-level)	7.1	<0.001	35.2 %
	te(Discharge, water-level)	11.9	<0.001	

6

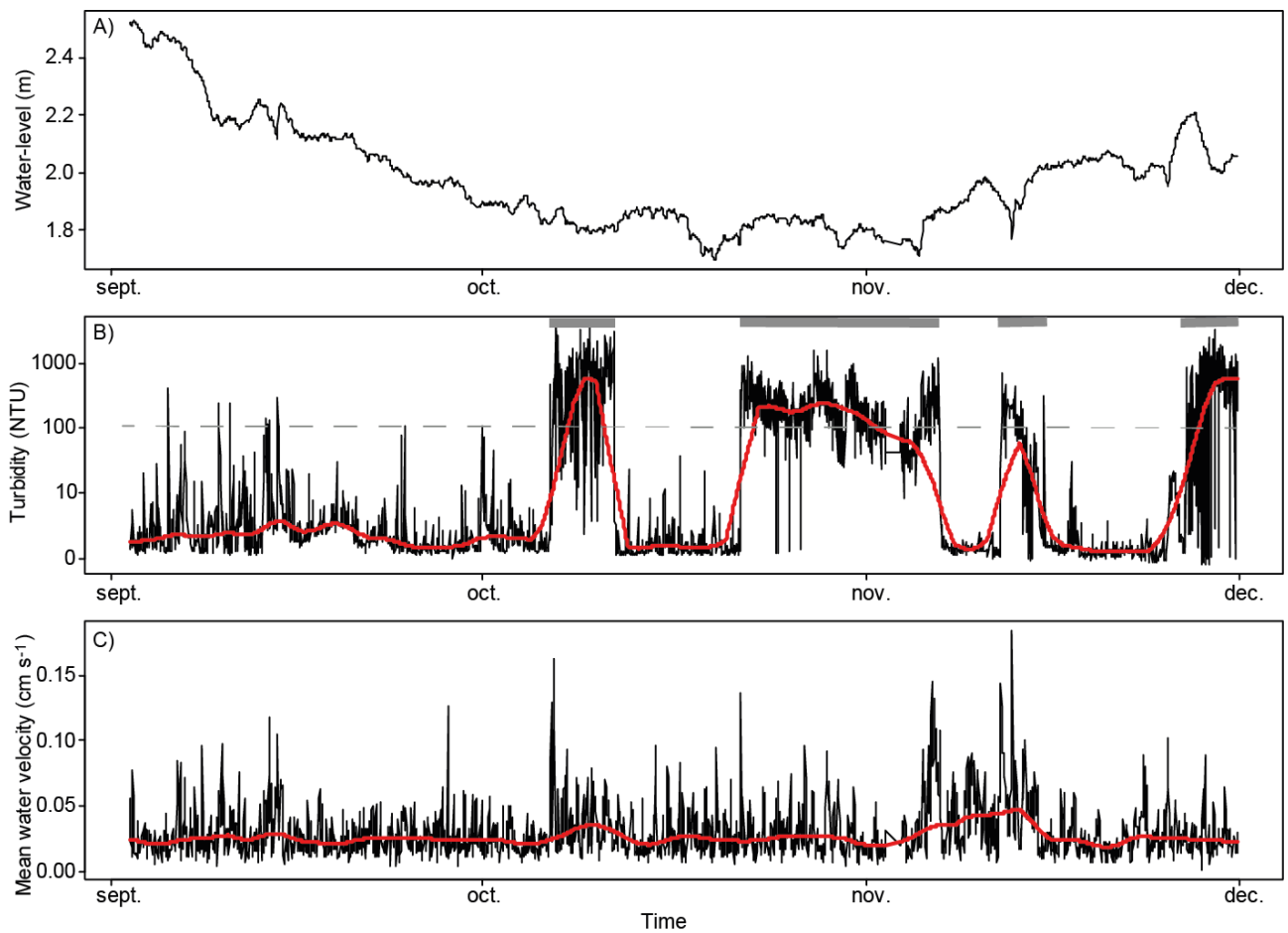
7

8

9

10 Figures

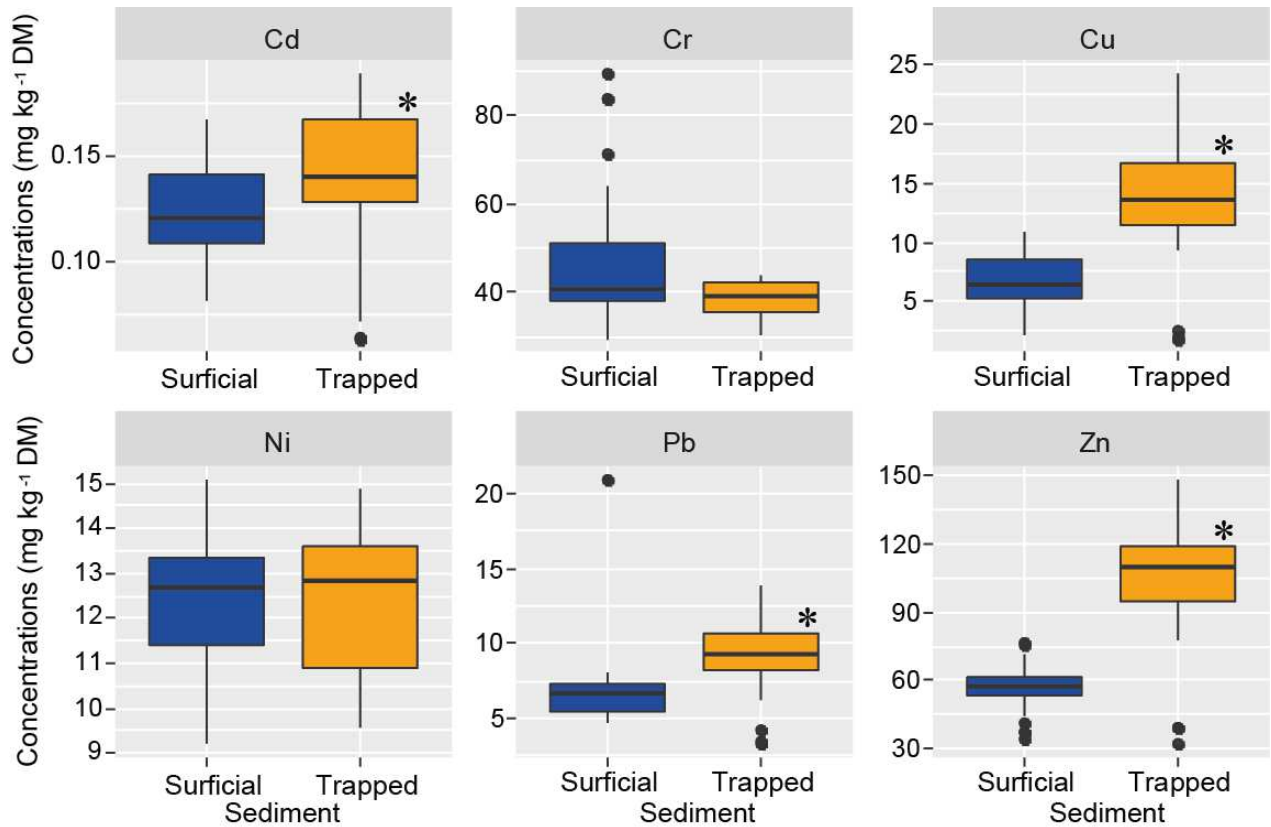
11



12

13 Figure 1: High-frequency dynamic of the littoral of Lake Bourget in autumn and winter 2017. A)  
14 water-level (m), B) turbidity (NTU, note the logarithmic-scale) and C) water velocity ( $\text{cm s}^{-1}$ ). Red  
15 lines represent Lowess-smooth trends (span window = 5% in the data,  $n = 2122$ ). The horizontal  
16 dashed grey line in B) indicates the threshold for a turbid event (turbidity higher than 100 NTU) and  
17 grey rectangles report the duration of the turbid events.

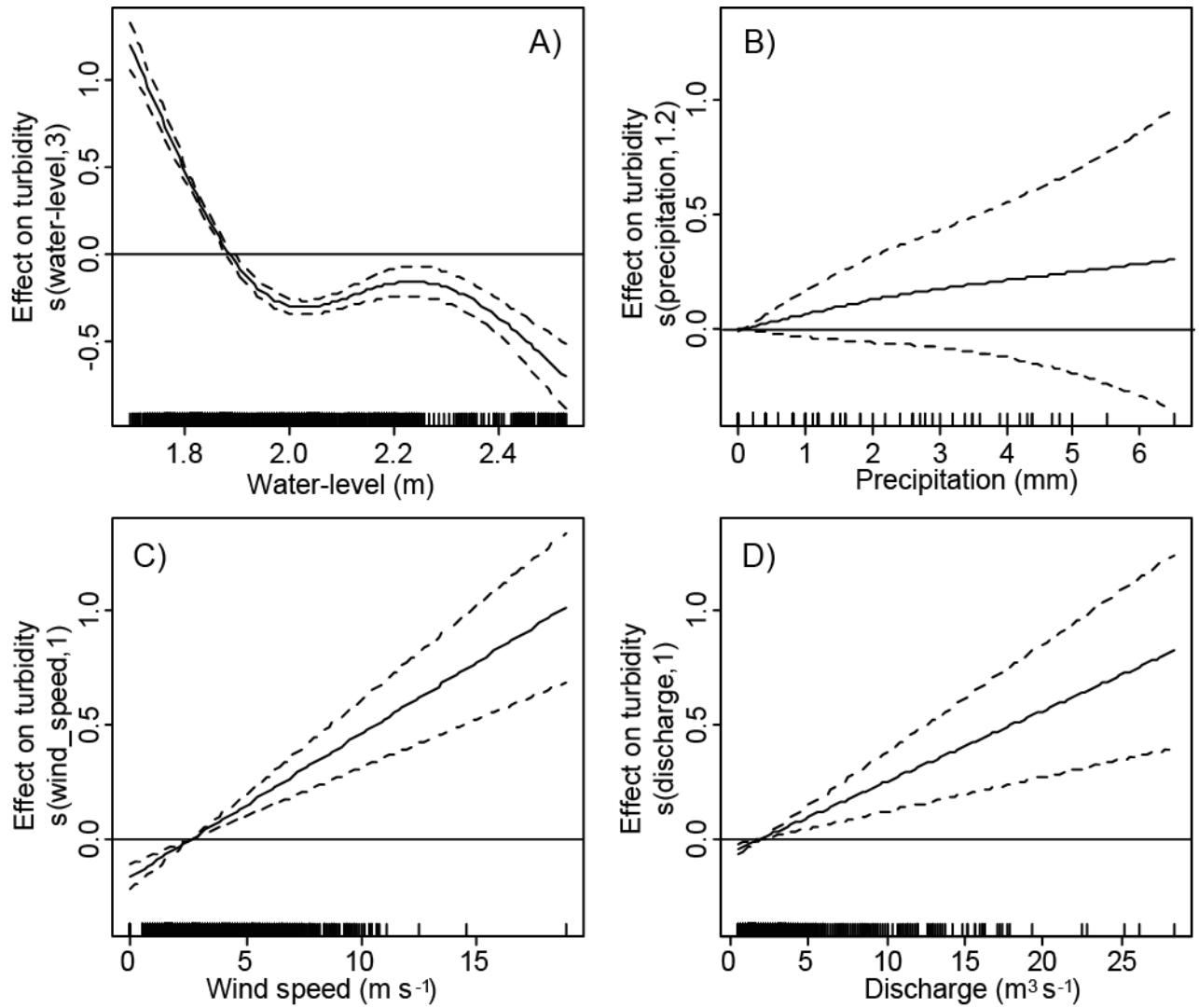
18



19

20 Figure 2: Boxplots of the trace metal concentrations (mg kg<sup>-1</sup> DM) in surficial (n = 27) and trapped (n  
 21 = 24) sediments. The water-level was too low at S<sub>0.7</sub> to enable trapped sediment sampling explaining  
 22 the lower sampling size of trapped sediment compared to surficial ones. The black stars indicate  
 23 significant differences in trace metal concentrations according to Mann-Whitney tests assuming a  
 24 significant threshold for p < 0.05.

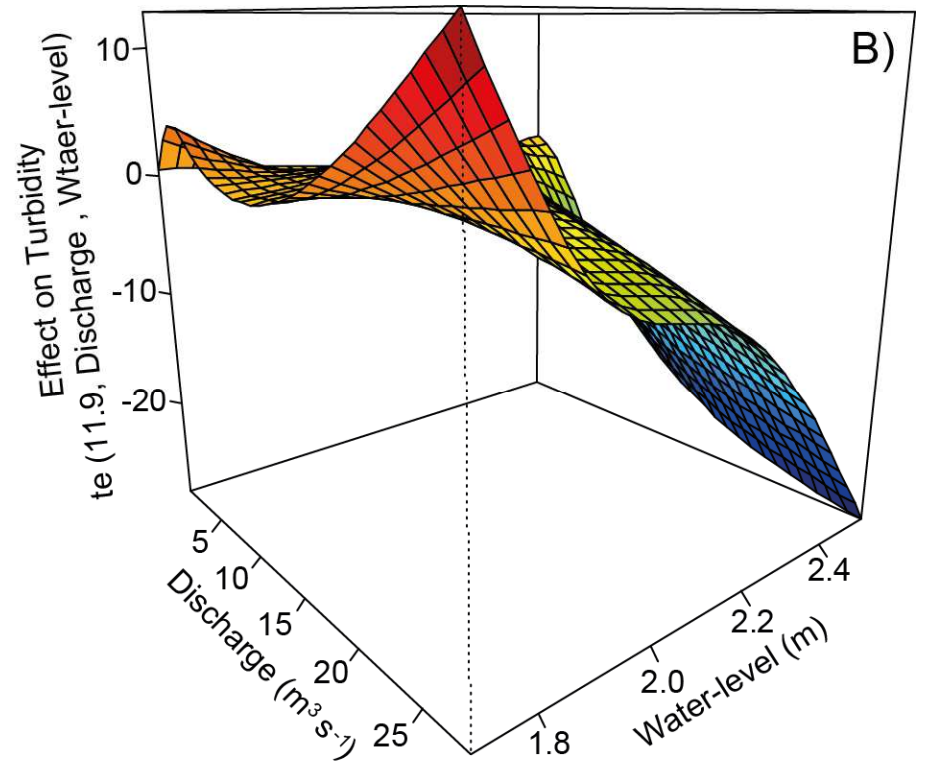
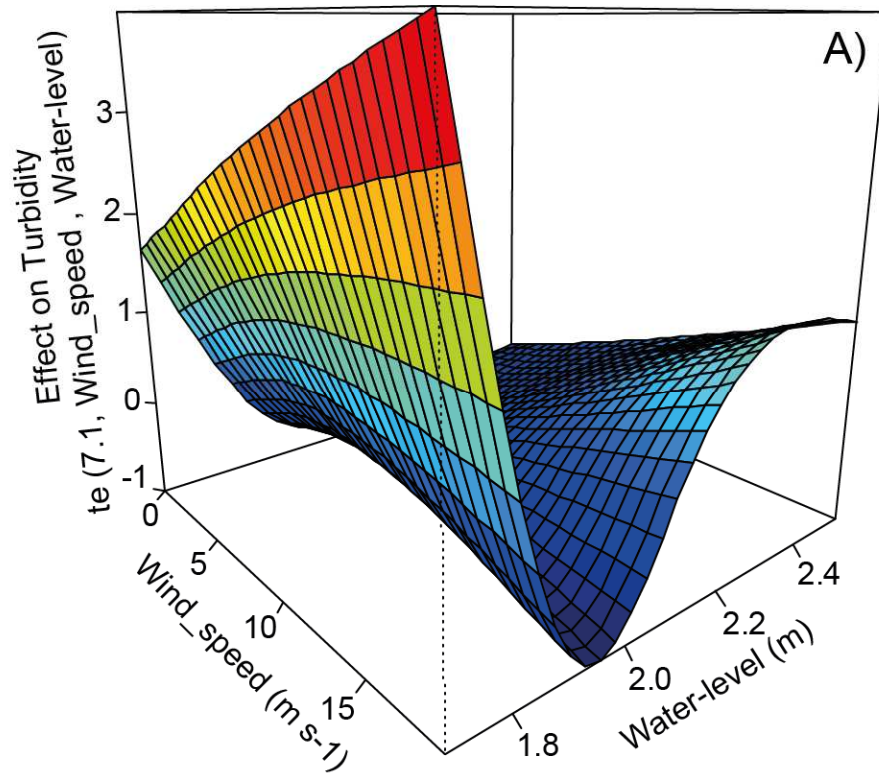
25



26

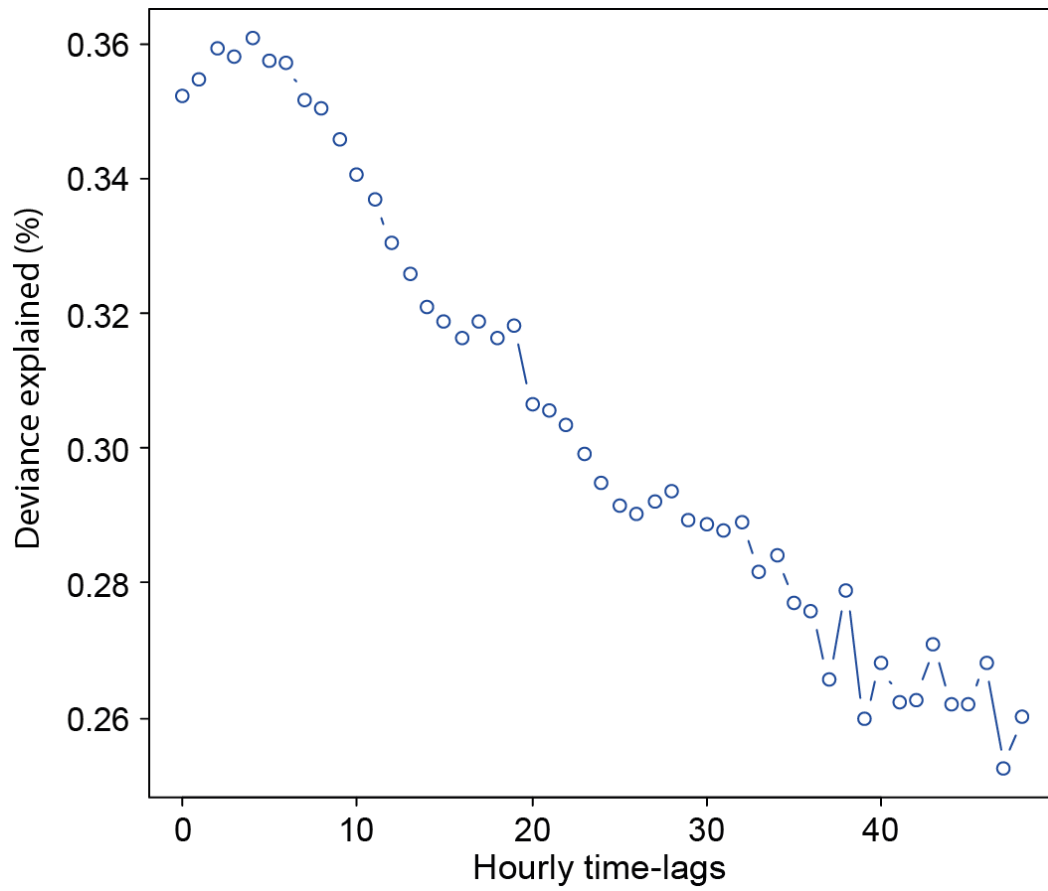
27 **Figure 3:** A) Smoothing of a simple GAM fitting the turbidity to WLF. Smoothings of a multivariate  
 28 GAM fitting the turbidity to B) precipitation, C) wind speed and D) discharge. The variable forcing  
 29 turbidity and the number referring to the edf (i.e. extent of nonlinear relationship) are indicated in  
 30 vertical brackets. The horizontal back lines indicate whether the variables have positive or negative  
 31 effects on turbidity.

32



33

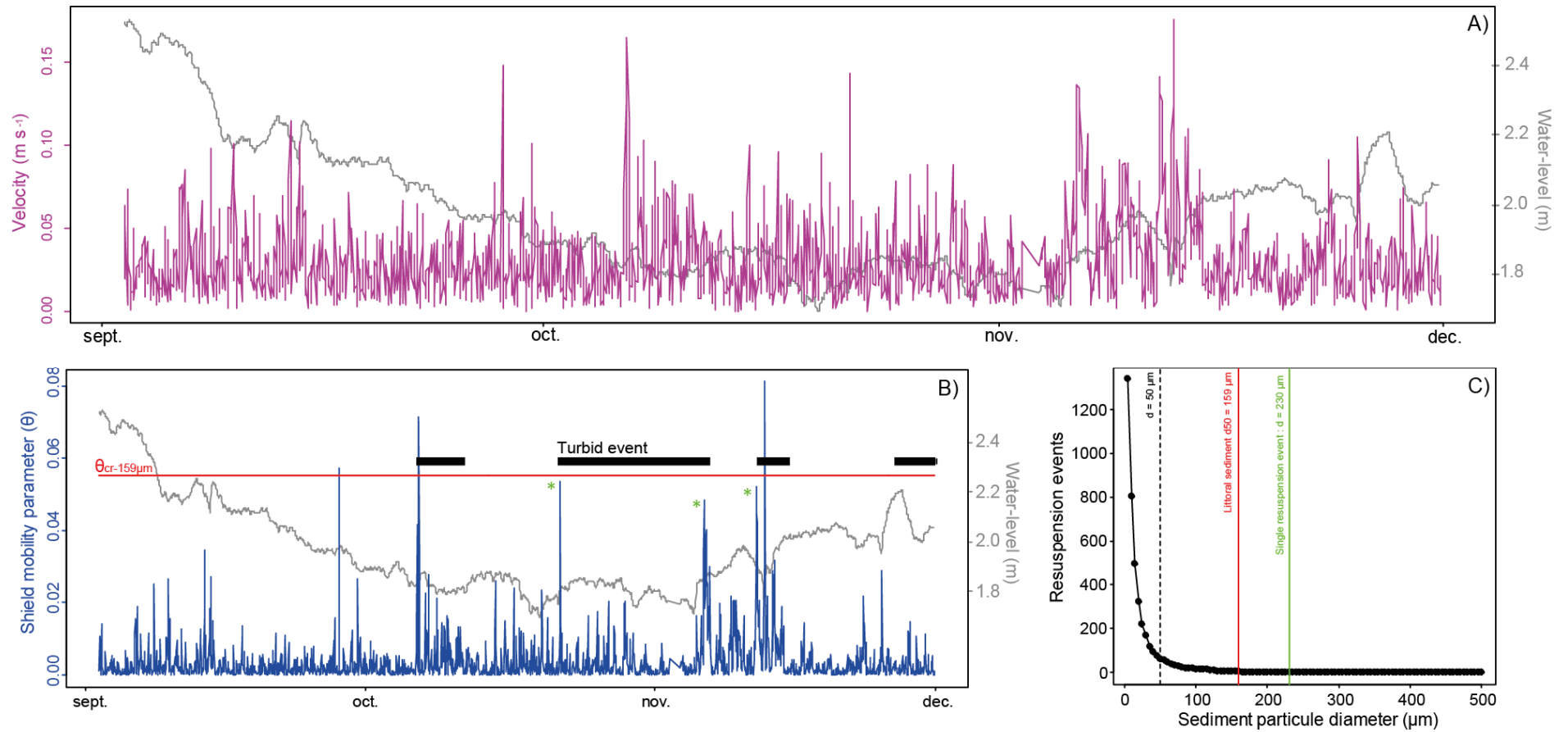
34 **Figure 4:** 3D-tensor product maps (i.e. interaction smooth functions) highlighting the implication of water-level at modulating the relationships between  
 35 turbidity and the external variables: A) wind speed ( $\text{m s}^{-1}$ ) and B) river discharge ( $\text{m}^3 \text{s}^{-1}$ ). The variable constraining turbidity and the number referring to the  
 36 edf (extent of nonlinear relationship) are reported in the vertical brackets.



38

39 [Figure 5](#): Changes in deviance explained of the GAM accounting for the interaction smooth  
40 functions over different hourly time-lags for the external forcings i.e. delayed effects of  
41 external forcings.

42



43

44 **Figure 6:** Sediment resuspension modeling: A) Dynamic of water velocity ( $\text{m s}^{-1}$ ). The grey line shows the water-level variations (m). B) Dynamic of the  
 45 Shield mobility parameter ( $\theta$ ). The horizontal red line shows the critical value for the resuspension of the mode grain size of lake sediment ( $\theta_{\text{cr-159}\mu\text{m}}$ , 159  $\mu\text{m}$   
 46 diameter). Green stars indicate additional resuspension events considering the mode grain size of trapped sediment (127  $\mu\text{m}$  diameter). The black rectangles  
 47 indicate the turbid events according to Fig. 1.B. C) Number of resuspension events according to sediment diameter ( $\mu\text{m}$ ). The vertical lines indicate sediment

48 diameters of interest:  $d = 230 \mu\text{m}$  is the maximal sediment diameter for the occurrence of a single resuspension event,  $d = 159 \mu\text{m}$  is the mode value for lake  
49 that encountered 3 resuspension events (see B of this figure) and  $d = 50 \mu\text{m}$ , below which resuspension events drastically increased, was submitted to 63  
50 resuspension events.